ECMS
2018

Effect of Silica Fume on the Pore Structure and Properties of Mortars Exposed to Sulphate Aggressive Media

José Marcos Ortega [1,2,*], María Dolores Esteban [2], Mark Williams [3], Isidro Sánchez [1] and Miguel Ángel Climent [1]

[1] Departamento de Ingeniería Civil, Universidad de Alicante, Ap. Correos 99, 03080, Alacant/Alicante, Spain; isidro.sanchez@ua.es (I.S.); ma.climent@ua.es (M.A.C.)
[2] Departamento de Ingeniería Civil, Urbanismo y Aeroespacial, Escuela de Arquitectura, Ingeniería y Diseño, Universidad Europea, c/ Tajo s/n, 28670, Villaviciosa de Odón, Madrid, Spain; mariadolores.esteban@universidadeuropea.es (M.D.E.)
[3] Engineeria, 7 Ridgmount Street, London, WC1E 7AE, U.K.; markmboro@gmail.com (M.W.)
[*] Correspondence: jm.ortega@ua.es; Tel.: +34-96-5903-400 (ext. 1167)

Abstract: The use of additions as clinker replacement has become very popular, due to the advantages that they provide, especially regarding the improvement of cement industry sustainability. The microstructure of cement-based materials has a direct influence on their service properties. In this research, mortars with different contents of silica fume (up to 10%) have been studied. These mortars were exposed to aggressive media with presence of sodium and magnesium sulphate along 90 days. On one hand, the evolution of their pore structure was characterised using different results provided by mercury intrusion porosimetry technique, such as intrusion-extrusion curves and logarithm of differential intrusion volume versus pore size curves. On the other hand, the compressive strength and the steady-state ionic diffusion coefficient obtained from resistivity of the samples, which was measured using impedance spectroscopy, were also studied. In general, silica fume mortars showed good performance, although the greatest deterioration of these mortars was observed in a mixed magnesium and sodium sulphate solution.

Keywords: silica fume; sulphate attack; sustainability; mercury intrusion porosimetry; ionic diffusion coefficient; mechanical strength.

1. Introduction

Nowadays, the use of additions in the cement production as clinker replacement has become very popular [1–6], because they provide several environmental benefits, such as the reduction of CO_2 emissions produced along the cement manufacture. Furthermore, most of these additions are residues which come from other industrial sectors, therefore their reuse also constitutes a benefit by itself.

One of the most used active additions is silica fume [7–10]. On one hand, it has been established by various authors that silica fume addition results in an improvement in durability related characteristics such as permeability [11–13], electrical resistivity [14,15] and chloride diffusivity [16–18]. These parameters are of fundamental importance as they affect the corrosion of reinforcing steel, which many authors consider to be the most severe pathology affecting reinforced concrete structures [19].

On the other hand, sulphate attack is another pathology which could produce deleterious effect in cement-based materials and structures. The classic harmful effects of this attack (ettringite and gypsum formation) are associated with the sulphate anion. It has been suggested that among the most typical associated cations, calcium and sodium are innocuous, while magnesium is aggressive

[19]. The chemical reactions produced by the sodium sulphate attack are shown in equations 1 and 2. The reaction of equation 2 produces the formation of expansive ettringite crystals.

$$Ca(OH)_2 + Na_2SO_4 + 2H_2O \rightarrow CaSO_4 \cdot 2H_2O + 2NaOH \quad (1)$$

$$3CaO \cdot Al_2O_3 + 3CaSO_4 \cdot 2H_2O + 26H_2O \rightarrow 3CaO \cdot Al_2O_3 \cdot 3CaSO_4 \cdot 32H_2O \quad (2)$$

The chemical reactions produced by the magnesium ion are shown in equations 3 and 4. The reaction shown in equation 3 results in the formation of magnesium hydroxide, or brucite, and is not greatly deleterious as calcium hydroxide does not contribute much to the strength of the hardened cement paste. The reaction shown in equation 4 is referred to as decalcification henceforth, and results in a severe loss of compressive strength due to the conversion of conglomerate calcium silica hydrate (C-S-H) gels into non-conglomerate magnesium silica hydrates(M-S-H) [20–22].

$$Mg^{2+} + Ca(OH)_2 \rightarrow Mg(OH)_2 + Ca^{2+} \quad (3)$$

$$Mg^{2+} + \text{C-S-H} \rightarrow \text{M-S-H} + Ca^{2+} \quad (4)$$

In relation to silica fume addition, it has been well documented that this addition increases resistance to sulphate ion attack, due to the consumption of portlandite during the pozzolanic reaction [23,24]. Then, as less portlandite is available to react with sulphate ions, fewer expansive reaction products (gypsum and ettringite) are formed. Other authors have observed experimentally that these results entailed a substantial reduction in expansion and a lower loss of compressive strength in silica fume blended cements [23–25].

However, when the associated cation is magnesium, the addition of silica fume has been shown to result in greater deterioration [24,26,27]. It has been agreed that this is a result of the lower availability of portlandite, which reacts with magnesium to form a double layer of brucite and gypsum, which was experimentally observed by Lee et al. (2005) [24]. This forms a barrier to the ingress of sulphate and magnesium ions, and additionally means that fewer magnesium ions are available to react with the hardened cement paste's calcium silica hydrate gels (so called "decalcification") [24]. The latter reaction is far more damaging, as the resulting magnesium silica hydrate gels are non-conglomerate. Decalcification therefore results in the disintegration of the hardened cement paste and an important loss of compressive strength.

Whereas the effects of reactions involving the sulphate anion have been extensively studied, the microstructural changes produced in the pore network have received less attention, especially in terms of porosity and pore size distribution. Furthermore, the current literature available does not consider the effects of microstructure deterioration resulting from exposure to either sulphate or magnesium ions on durability characteristics and mechanical properties, although some authors have noted small decreases in porosity during the initial phases of sulphate ion attack [28].

Then, the main purpose of the present paper is to investigate the effect of exposure to magnesium and sodium sulphate solutions on the microstructure and properties of mortars with different contents of silica fume, compared to mortars containing ordinary Portland cement only. Moreover, this study complements two previous authors' works [29,30] in which several types of sustainable mortars and grouts with silica fume exposed to sulphate attack were studied.

2. Materials and Methods

2.1. Sample Preparation and Curing

Three types of mortars were analysed. For all of them the cement used was a high early strength type, belonging to European cement class CEM I 42.5 R [31]. The first type of mortar had no addition of silica fume (referred to as 0% silica fume mortar hereafter), and it was used as a pattern for performance. Apart from that, two mortars in which 5% and 10% of cement was replaced with silica fume were also studied (designated as 5% silica fume and 10% silica fume mortars respectively from now on). The silica fume used was not densified, with 90.78% of its particles under 1 μm and an average particle diameter of 0.67 μm. The chemical composition of the materials and calculated clinker compounds of the cement are shown in Table 1. The fine aggregate to binder ratio was 3:1 and the water to binder ratio was 0.5, as prescribed by standard UNE-EN 196-1 [32]. Cylindrical (10 cm diameter and 15 cm height) and prismatic (4 cm x 4 cm x 16 cm) specimens were made. The samples were cured for 7 days in a temperature and humidity controlled chamber at 20º C and 95% relative humidity (RH). Following this period they were de-moulded, cut to shape as required, and introduced into the corresponding sulphate solution. In particular, the cylindrical specimens were cut in 2 cm thick slices, and the prismatic samples were divided in three identical elements whose dimensions were 4 cm x 4 cm x 5.3 cm. The samples were tested at different times, until 90 days of contact with the sulphate solutions.

Table 1. Chemical composition of the cement and silica fume.

Compound	CEM I 42.5R (%)	Silica Fume (%)
CaO	64.5	0.4
SiO_2	20.0	94.1
Al_2O_3	5.7	0.3
Fe_2O_3	2.5	0.1
SO_3	3.2	0.1
MgO	0.9	0.3
Na_2O	0.1	0.6
K_2O	1.0	0.6

2.2. *Sulphate Solutions*

The specimens were exposed to three sulphate solutions. The sulphate solutions used consisted of combinations of reagent grade magnesium sulphate ($MgSO_4$) and sodium sulphate (Na_2SO_4) dissolved in distilled water, and changed once after 45 days. The content in sulphate and magnesium ions present in each solution is shown in Table 2. Each solution is denominated by the percentage by weight of dissolved sulphates. The volume of solutions was approximately 4 times the volume of the samples, as is suggested by the ASTM C 1012-04 standard [33]. Finally, the relatively high concentration of sulphate (15%) was chosen for speeding up the harmful effects produced by this aggressive ion, in order to note them at short exposure times.

Table 2. Content in aggressive ions and ratio of magnesium to sulphate ions in the sulphate solutions used.

Solution Name	Mg^{2+} (g/l)	SO_4^{2-} (g/l)	Mass Ratio Mg^{2+}/SO_4^{2-}	Mg^{2+} (mol/l)	SO_4^{2-} (mol/l)	Molar ratio Mg^{2+}/SO_4^{2-}
15% Na_2SO_4	0	101.442	0	0	1.056	0
7.5% $MgSO_4$ + 7.5% Na_2SO_4	15.145	110.576	0.136	0.621	1.151	0.539
15% $MgSO_4$	30.290	119.710	0.253	1.246	1.246	1.000

2.3. *Mercury Intrusion Porosimetry*

A porosimeter model AUTOPORE IV 9500 of Micromeritics (Norcross, GA, USA) was used. The apparatus allowed the determination of the volume of pores with an accessible diameter of 5 nm to 900 μm. The samples were taken from slices with 2 cm thickness, and they were dried in an oven at 50°C along one week before testing. Two measurements were performed for each material, solution and testing age. The intrusion-extrusion curves, the curves logarithm of differential intrusion volume versus pore size and the median pore diameter were analysed. The tests were made at 21 and 90 days of exposure to the different studied solutions.

2.4. Determination of Steady-State Ionic Diffusion Coefficient from Resistivity of Sample Obtained Using Impedance Spectroscopy

The electrical resistivity measurement of a cement-based material is an indirect method to assess their pore connectivity and determine the ionic steady-state diffusion coefficient D_s [34]. Here, the electrical resistivity was calculated from the electrical resistance of the specimens immersed in the sulphate solutions, using the non-destructive impedance spectroscopy technique [35–37]. This technique has successfully been used in several previous authors' researches for characterising the pore network of cement-based materials with silica fume [29,30] and other active additions [38,39].

In the current work, the impedance measurements were carried out in 2 cm thick slices using an impedance analyzer Agilent 4294A (Agilent Technologies, Kobe, Japan), capable of capacitance measurements in the 10^{-14} – 0.1 F range, with a maximum resolution of 10^{-15} F. Circular copper electrodes with a flexible graphite contact surface and a diameter of 8 cm were used, and measurements were taken over a frequency range of 100 Hz to 100 MHz. The electrodes were placed in direct contact with the samples during measurement. The obtained spectra were fitted to the equivalent circuit proposed by Cabeza et al. [36] (see Figure 1) using a simplex algorithm, described elsewhere [40]. One of the circuital elements is the resistance R_1 (see Figure 1), which is associated with pores that cross the sample. This resistance R_1 is equivalent to the electrical resistance of the sample [41,42].

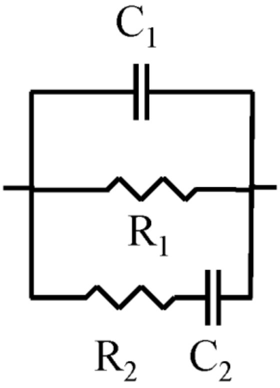

Figure 1. Equivalent circuit used for the fitting of the impedance spectra obtained using the contacting method, in which the resistance R_1 is associated with pores that cross the sample.

The steady-state ionic diffusion coefficient (D_s) was calculated according to the expression proposed by Andrade et al. [34], shown in equation 5, in which the coefficient D_s is expressed in m²/s, and the electrical resistivity ϱ in Ω·m.

$$D_s = \frac{2 \times 10^{-10}}{\rho} \quad (5)$$

For each mortar type and solution four different samples were tested. The variation in steady-state ionic coefficient was followed up to 90 days of exposure to the sulphate solutions.

2.5. Compressive Strength

The compressive strength was determined according to the Spanish standard UNE-EN 196-1 [32], in prisms of dimensions 4 cm × 4 cm × 5.3 cm. Three different samples were tested for each mortar type and solution. This parameter was obtained at 21 and 90 days of exposure to the sulphate solutions.

3. Results and Discussion

3.1. Mercury Intrusion Porosimetry

The intrusion-extrusion curves for samples exposed to the 15% Na_2SO_4 solution are depicted in Figure 2 and their median pore diameters are noted in Table 3. It may be noted that in the 0% silica fume samples, the total intrusion volume increased very slightly with exposure period, increasing by less than 1% from 21 days to 90 days exposure. For the median pore diameter an increase was observed. Some variations were also observed in the values recorded in the 5% and 10% silica fume samples. For 5% silica fume specimens, a slight increase in the total intrusion volume has been noted, as well as for the median pore diameter. In the case of 10% silica fume samples, the total intrusion volume slightly decreased from 21 to 90 days, and the median pore diameter rose in this period. The lowest increase of this parameter between 21 and 90 days has been observed for 10% silica fume specimens, followed by 5% silica fume ones. On the other hand, for the 15% Na_2SO_4 solution the highest increase of the median pore diameter along the studied period corresponded to 0% silica fume samples.

The intrusion-extrusion curves for samples exposed to the mixed solution are shown in Figure 3 and their median pore diameters can be observed in Table 3. The total intrusion volume was relatively unaffected by exposure to this 7.5% $MgSO_4$ + 7.5% Na_2SO_4 solution in the 0% and 10% silica fume samples, and that a reduction was observed with exposure period in the 5% silica fume samples. A reduction of the median pore diameter was observed for 5% silica fume specimens, and this parameter increased for 0% and 10% silica fume ones, being this rise very important for the last type of samples.

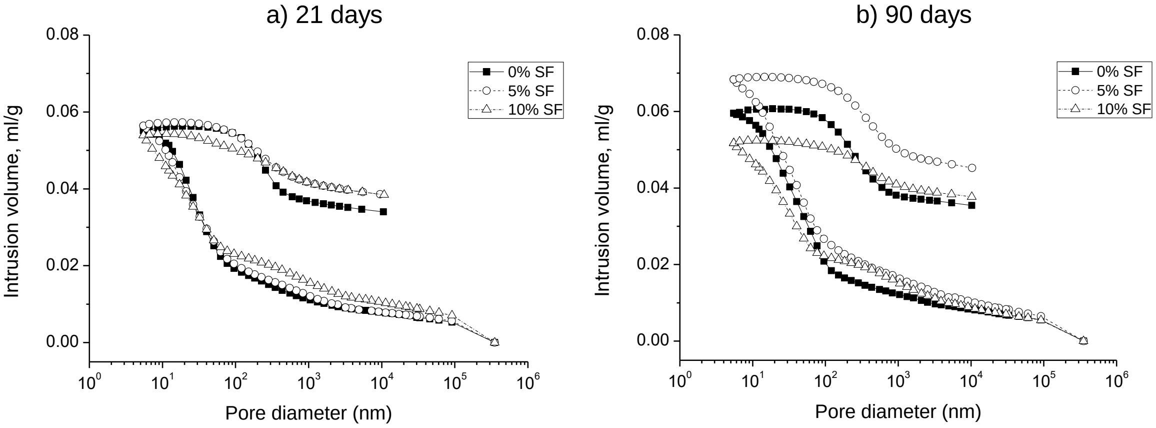

Figure 2. **(a)** Intrusion-extrusion curves at 21 days of exposure to the 15% Na_2SO_4 solution for mortars prepared using ordinary Portland cement without addition (0% SF), and for those with a content of 5% (5% SF) and 10% (10% SF) of silica fume; **(b)** Intrusion-extrusion curves at 90 days of exposure to the 15% Na_2SO_4 solution noted for the studied mortars.

Regarding the samples exposed to the 15% $MgSO_4$ solution, their intrusion-extrusion curves can be observed in Figure 4, while their median pore diameters are included in Table 3. Scarce differences were observed between the different types of studied samples in relation the total intrusion volume. However, the median pore diameter rose with time for all the studied samples, and this increase is higher as greater is the content of silica fume, being especially noticeable for specimens with a 10% content of this addition.

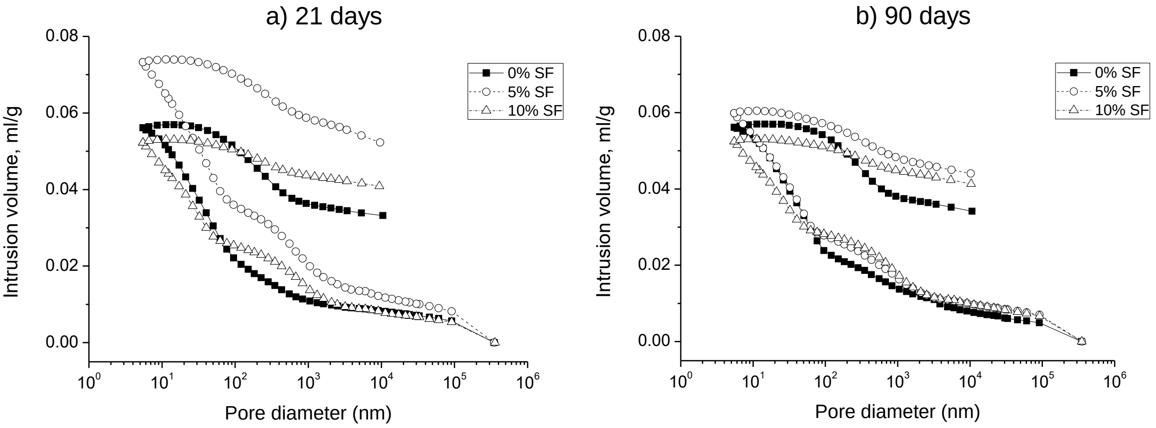

Figure 3. **(a)** Intrusion-extrusion curves at 21 days of exposure to the mixed solution (7.5% Na_2SO_4 + 7.5% $MgSO_4$) for the analysed mortars; **(b)** Intrusion-extrusion curves at 90 days of exposure to the mixed solution (7.5% Na_2SO_4 + 7.5% $MgSO_4$) obtained for the studied mortars.

Table 3. Median pore diameter (nm) measured for the studied mortars.

Mortar	15% Na_2SO_4 solution			Mixed solution			15% $MgSO_4$ solution		
type	21 days	90 days	Variation	21 days	90 days	Variation	21 days	90 days	Variation
0% SF	43.3	58.8	35.8%	58.8	68.8	17.0%	60.8	67.5	11.0%
5% SF	44.4	55.6	25.2%	86.3	64.6	-25.1%	79.7	97.5	22.3%
10% SF	48.8	54.3	11.3%	72.3	216.1	198.9%	79.6	289.2	263.3%

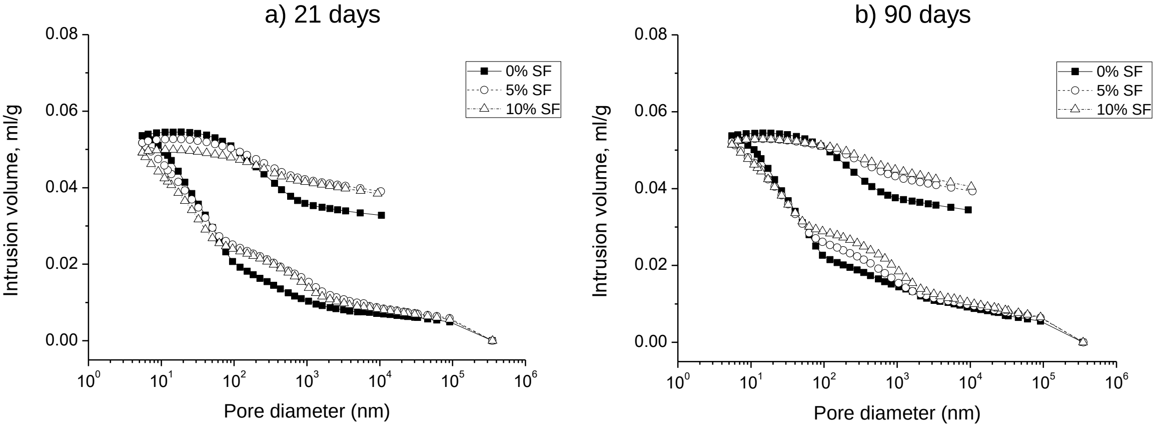

Figure 4. **(a)** Intrusion-extrusion curves at 21 days of exposure to the 15% $MgSO_4$ solution for the studied mortars; **(b)** Intrusion-extrusion curves at 90 days of exposure to the 15% $MgSO_4$ solution noted for the studied mortars.

The curves logarithm of differential intrusion volume versus pore size obtained for the samples exposed to the 15% Na_2SO_4 solution at 21 and 90 days are shown in Figure 5. In the 0% silica fume samples, the principal effect appears to be on the pore family whose centre is at around $2 \cdot 10^1$ nm. At 90 days, a widening of this pore family may be observed and now the main peak of this family is around 10^2 nm. This would indicate a loss of pore refinement for 0% silica fume samples which could be due to the development of sulphate attack [29,30]. At 21 days the samples containing silica fume both showed two peaks in the range 10^1-10^2 nm, which merged in one peak at 90 days, whose diameter was lower than that noted for 0% silica fume specimens. This result is consistent with the established idea that samples containing silica fume show a more refined pore structure, and in agreement with results presented by other authors [13,16,43]. Furthermore, in view of the differential intrusion volume, the samples containing 10% silica fume appear not to have been greatly affected between 21 and 90 days exposure, while the 5% silica fume sample showed a greater volume of pores present in the abovementioned pore family.

In Figure 6 it can be observed the curves logarithm of differential intrusion volume versus pore size obtained for the samples exposed to the mixed solution. From this figure, the principal pore family (between 10^1 and 10^2 nm) for the 0% silica fume samples was relatively unaffected, although the main peak in the previously mentioned range moved to higher diameters from 21 to 90 days, and a small peak appeared at approximately $3·10^3$ nm. For samples containing silica fume, apart from the family in the range 10^1 and 10^2 nm, a prominent pore family centred at around 10^3 nm was observed, which was not registered in the samples exposed to the 15% Na_2SO_4 solution. This would mean that the microstructure of silica fume mortars would be more affected by the exposure to the mixed solution than by the sodium sulphate one, as suggested the loss of pore refinement indicated by this new pores family with higher diameter. Slight changes has been noted in the pore families observed for silica fume specimens from 21 days to 90 days, although it may be observed that the 10% silica fume samples' principal pore family showed a small decrease.

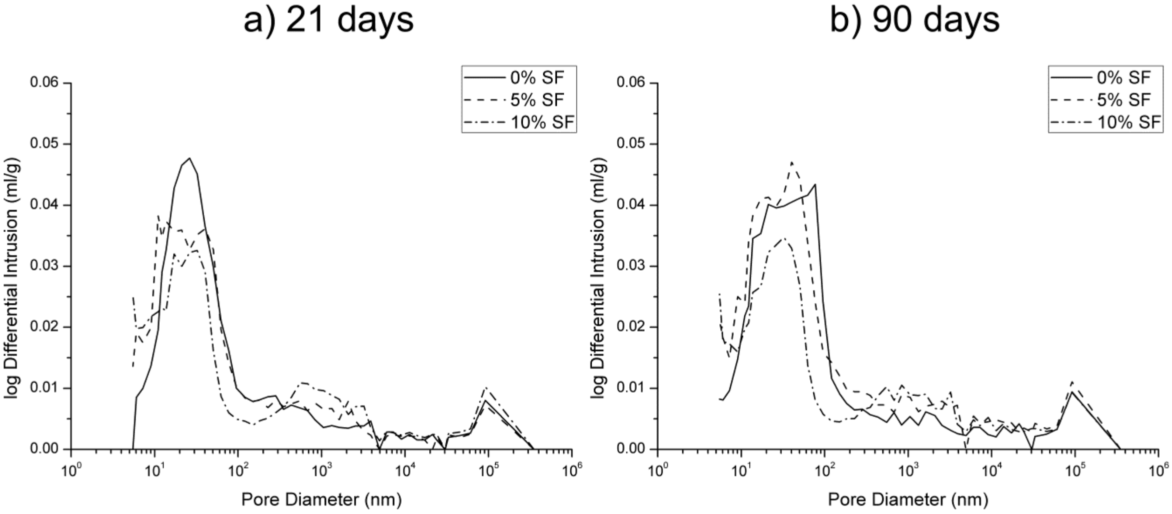

Figure 5. **(a)** Curves logarithm of differential intrusion volume versus pore size obtained at 21 days of exposure to the 15% Na_2SO_4 solution; **(b)** Curves logarithm of differential intrusion volume versus pore size obtained at 90 days of exposure to the 15% Na_2SO_4 solution.

In relation to the curves logarithm of differential intrusion volume versus pore size noted for the samples exposed to the 15% $MgSO_4$ solution (see Figure 7), they showed similarities to those observed for the mixed solution. For 0% silica fume samples, the main pores family was again in the interval 10^1-10^2 nm, although at 90 days a noticeable peak appeared approximately at $2·10^3$ nm, as happened for the mixed solution. For 5% and 10% silica fume specimens the same prominent pore family at around 10^3 nm was present and it slightly increased in size between 21 and 90 days exposure. This appears to suggest that the formation of this pore family resulted from the deterioration processes associated with the magnesium ion [24,27], as it was not observed in the samples exposed to the 15% Na_2SO_4 solution. Regarding the main peak of the range 10^1-10^2 nm for the silica fume mortars, it slightly displaced to greater pore sizes between 21 and 90 days, which would show the deleterious effects of the $MgSO_4$ solution in their microstructure [26,27].

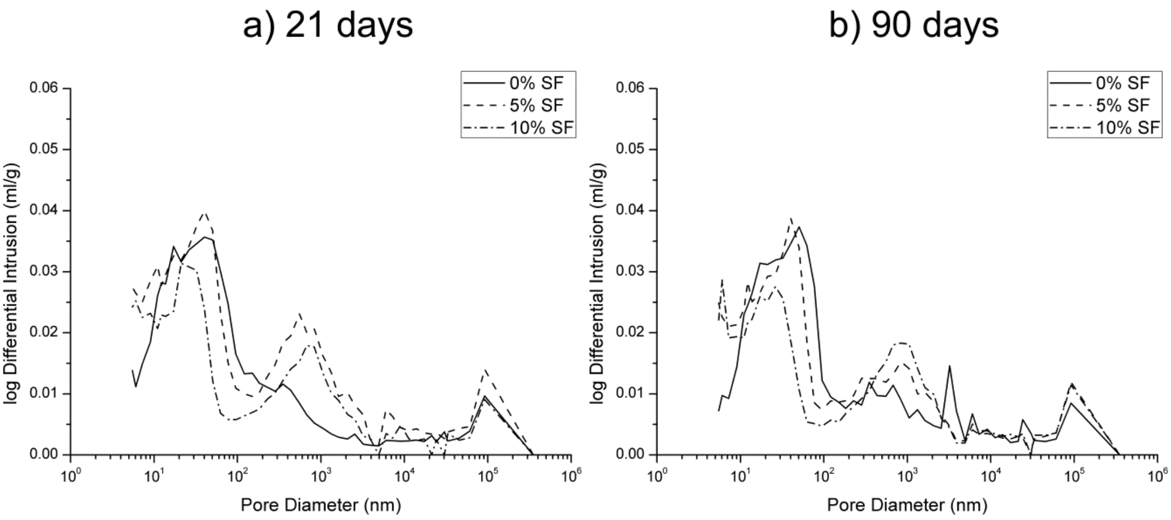

Figure 6. **(a)** Curves logarithm of differential intrusion volume versus pore size showed by the studied mortars at 21 days of exposure to the mixed solution; **(b)** Curves logarithm of differential intrusion volume versus pore size showed by the studied mortars at 90 days of exposure to the mixed solution.

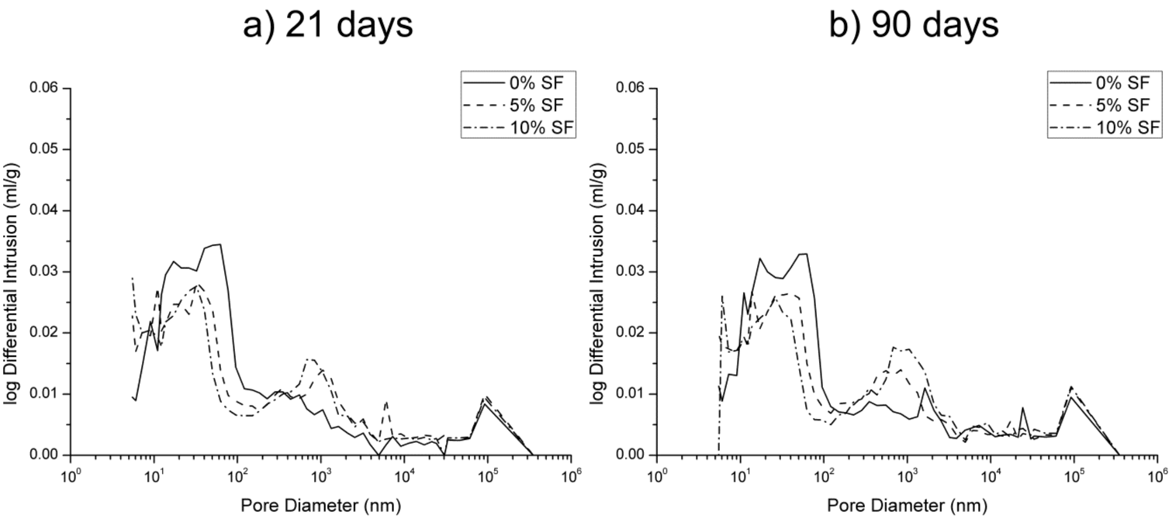

Figure 7. **(a)** Curves logarithm of differential intrusion volume versus pore size obtained at 21 days of exposure to the 15% $MgSO_4$ solution; **(b)** Curves logarithm of differential intrusion volume versus pore size obtained at 90 days of exposure to the 15% $MgSO_4$ solution.

3.2. Steady State Ionic Diffusion Coefficient

The changes with time in the steady state ionic diffusion coefficient (D_s) measured in samples exposed to the 15% Na_2SO_4 solution can be observed in Figure 8. This figure shows firstly that, in agreement with the published literature discussed previously [16–18], the steady state ionic diffusion coefficient (D_s) decreased with silica fume content. Additionally, exposure to the 15% Na_2SO_4 solution appears not to have produced any increase in D_s, which suggests that the sulphate resistance of the samples containing silica fume was high. In fact, the silica fume samples showed a relatively constant reduction in D_s, which may have been linked to the continued pozzolanic reaction of the silica fume present. No increase in D_s was observed in the 0% silica fume samples, implying that sulphate attack did not affect this parameter, at least during the relative short time period studied.

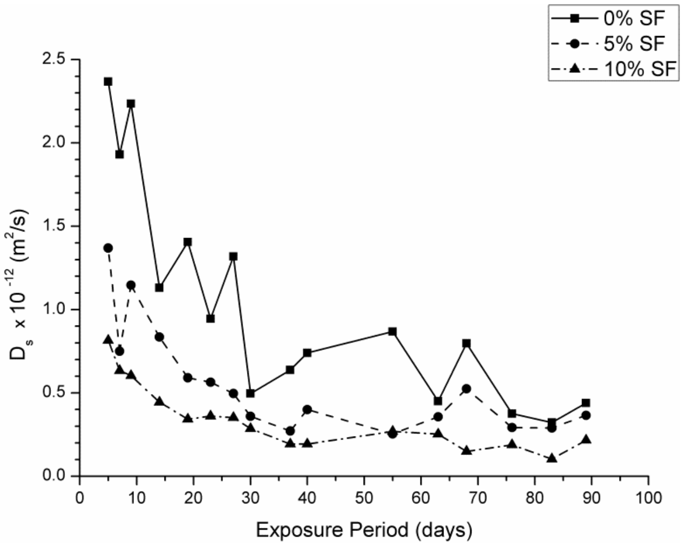

Figure 8. Variation in the steady state ionic diffusion coefficient (D_s) measured in samples exposed to the 15% Na_2SO_4 solution.

Regarding the 7.5% $MgSO_4$ + 7.5% Na_2SO_4 solution, it may be observed from Figure 9 that the samples containing 0% silica fume show a similar reduction in D_s to that observed in the 15% Na_2SO_4 solution. This may be as a result of the formation of a double layer of brucite and gypsum, as discussed previously [24]. However, both the samples containing 5% and 10% silica fume showed an increase in D_s after an initial decrease (probably associated with the initial pozzolanic hydration of the silica fume). This suggests that exposure to the 7.5% $MgSO_4$ + 7.5% Na_2SO_4 solution resulted in deterioration in these samples, which could be very severe in the long-term. It may be noted, for instance, that in the 10% silica fume sample, D_s was greater by the end of the exposure period than the initial value recorded at a sample age of 11 days (4 days exposure).

This deterioration was likely as a result of decalcification reactions, as observed by other authors [20–22]. The conversion of C-S-H gels to non-conglomerate M-S-H gels within the pore network would plausibly have the effect of dissolving hardened cement paste, decreasing the tortuosity of the pore network and increasing the porosity. As such, it may be inferred that exposure to magnesium ions increases ionic diffusivity in samples containing silica fume. It is also significant that by the end of the test period, the values of D_s measured in the samples containing silica fume were almost double those measured in the sample containing Portland cement only.

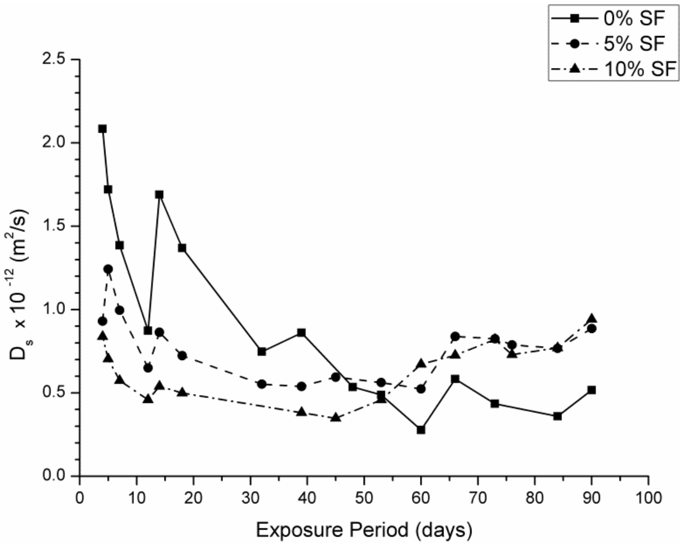

Figure 9. Variation in the steady state ionic diffusion coefficient (D_s) measured in samples exposed to the mixed solution.

However, the results of the steady state ionic diffusion coefficient (D_s) measured in the samples exposed to the 15% $MgSO_4$ solution, presented in Figure 10, somewhat conflict with the idea that it is purely the action of the magnesium ion that causes an increase in D_s. Despite the fact that the samples shown in that figure were exposed to the 15% $MgSO_4$ solution with the highest concentration of magnesium ions (see Table 2), the value of D_s remained relatively constant in the 5% silica fume samples, and in the 10% silica fume samples it increased only slightly with exposure period compared to the lowest D_s value noted. This appears to suggest that changes in the ionic diffusivity in silica fume samples are not directly proportional to the concentration of magnesium ions present. It would hence appear that the deterioration mechanism is more complex than previously assumed.

The 0% silica fume samples exposed to the 15% $MgSO_4$ solution showed a relatively constant decrease in D_s. It may be noted that in all of the solutions, the values of D_s were very similar by the end of the exposure period, despite some differences in the initial values. These results appear to suggest that in non-blended cements, sulphate attack does not result in significant changes in the steady state ionic diffusion coefficient. However, it should be noted that the solutions used were extremely concentrated and the test period was short (90 days), and as such further research is necessary to confirm this assertion.

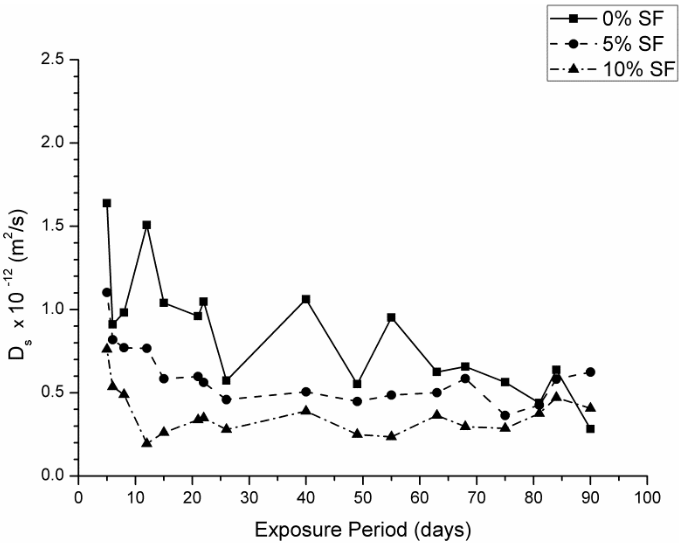

Figure 10. Variation in the steady state ionic diffusion coefficient (D_s) measured in samples exposed to the 15% $MgSO_4$ solution.

3.3. Compressive Strength

The compression strength results and its variation in percentage between 21 and 90 exposure days are shown in Table 4 for all the samples and solutions studied. In that table, it may be observed that exposure to the Na_2SO_4 solution did not result in any substantial reduction in compressive strength in the samples containing both 5% and 10% silica fume, even this parameter slightly increased for them, but a significant reduction of 34.4% was observed in the 0% silica fume samples. This correlates well with data available in current literature [23,24,26,44], and is probably due to the silica fume samples having substantially less portlandite available for reaction with the sulphate ions present in solution, as discussed previously.

It may be inferred from the compressive strength results that exposure to the 7.5% $MgSO_4$ + 7.5% Na_2SO_4 solution resulted in severe deterioration (likely due to decalcification [20–22]) in both of the samples containing silica fume. However, the samples without silica fume showed relatively little deterioration in terms of compressive strength. In addition, the results of this parameter suggests that in the samples containing 0% silica fume, exposed to the 15% $MgSO_4$ solution resulted in least deterioration of all samples. In fact, there was actually an increase in compressive strength.

Despite the total concentration of magnesium ions being highest in the 15% $MgSO_4$ solution, the loss of compressive strength observed in the silica fume samples was not as severe as that which occurred in those exposed to the 7.5% $MgSO_4$ + 7.5% Na_2SO_4 solution (see Table 4). This suggests that the deterioration mechanism responsible for the reduction in compressive strength in the silica fume samples does not depend solely on the concentration of magnesium ions present. It also appears that the extent of deterioration in the samples containing silica fume was less than that observed by other authors using weaker $MgSO_4$ solutions [16,27,45]. It is hence possible that the use of a more concentrated solution and a shorter test period does not produce the same results.

Table 4. Compressive strength (MPa) results obtained for the studied mortars.

Mortar	**15% Na_2SO_4 solution**			**Mixed solution**			**15% $MgSO_4$ solution**		
type	**21 days**	**90 days**	**Variation**	**21 days**	**90 days**	**Variation**	**21 days**	**90 days**	**Variation**
0% SF	32.3	21.2	-34.4%	36.5	34.9	-4.4%	36.5	40.8	11.8%
5% SF	57.9	59.9	3.5%	53.0	44.2	-16.6%	46.2	47.4	2.6%
10% SF	63.3	67.5	6.6%	59.2	45.1	-23.8%	56.0	53.1	-5.2%

4. Conclusions

The main conclusions that can be drawn from the previously discussed results can be summarized as follows:

- The pore structure of 0% silica fume samples exposed to sodium sulphate solution was less refined compared to 5% and 10% silica fume ones. This would indicate that the silica fume inclusion improves the resistance to sodium sulphate attack in mortars.
- The microstructure of silica fume mortars was more affected by the exposure to the mixed 7.5% $MgSO_4$ + 7.5% Na_2SO_4 solution than by the sodium sulphate one, as suggested the loss of pore refinement indicated by the appearance of a new pore family with higher diameter. A similar result has been noted for magnesium sulphate solution.
- The steady state ionic diffusion coefficient decreases with silica fume content, and appears not to be affected by exposure to sodium sulphate solutions.
- In silica fume samples exposed to magnesium sulphate solutions, a substantial increase in ionic diffusivity accompanies a loss in compressive strength, suggesting that dissolution type reactions take place in these samples pore network. This attack was more severe in the 7.5% $MgSO_4$ + 7.5% Na_2SO_4 solution, which implies that magnesium content alone does not determine the severity of attack.

Acknowledgments: The research work included in the paper has been financially supported by the University of Alicante (Spain) through project GRE13-25. The authors also wish to thank Cementos Portland Valderrivas S.A. and Grupo Ferroatlántica, S.A. for providing the cement and silica fume (respectively) used in this study.

Author Contributions: José Marcos Ortega and Mark Williams wrote the paper. José Marcos Ortega, Mark Williams and Isidro Sánchez performed the experiments. María Dolores Esteban and Miguel Ángel Climent supervised the research work and revised the paper. All the authors contributed to conceive and design the experiments, and to analyse and discuss the results.

Conflicts of Interest: The authors declare no conflict of interest.

References

1. Demirboğa, R. Thermal conductivity and compressive strength of concrete incorporation with mineral admixtures. *Build. Environ.* **2007**, *42* (7), 2467–2471 DOI: 10.1016/j.buildenv.2006.06.010.
2. Ganjian, E.; Pouya, H. S. The effect of Persian Gulf tidal zone exposure on durability of mixes containing silica fume and blast furnace slag. *Constr. Build. Mater.* **2009**, *23* (2), 644–652 DOI:

10.1016/j.conbuildmat.2008.02.009.

3. Ponikiewski, T.; Gołaszewski, J. The effect of high-calcium fly ash on selected properties of self-compacting concrete. *Arch. Civ. Mech. Eng.* **2014**, *14* (3), 455–465 DOI: 10.1016/j.acme.2013.10.014.
4. Ortega, J. M.; Sánchez, I.; Climent, M. A. Impedance spectroscopy study of the effect of environmental conditions in the microstructure development of OPC and slag cement mortars. *Arch. Civ. Mech. Eng.* **2015**, *15* (2), 569–583 DOI: 10.1016/j.acme.2014.06.002.
5. Glinicki, M.; Jóźwiak-Niedźwiedzka, D.; Gibas, K.; Dąbrowski, M. Influence of Blended Cements with Calcareous Fly Ash on Chloride Ion Migration and Carbonation Resistance of Concrete for Durable Structures. *Materials (Basel).* **2016**, *9* (1), 18 DOI: 10.3390/ma9010018.
6. Ortega, J.M.; Sánchez, I.; Climent, M.A. Influence of environmental conditions on durability of slag cement mortars. In: Zachar, J., Claisse, P., Naik, T.R., Ganjian, E. (Eds.), Proceedings of the 2nd International Conference on Sustainable Construction Materials and Technologies, pp. 277–287, Ancona, Italy, 28–30 June 2010.
7. Nochaiya, T.; Wongkeo, W.; Chaipanich, A. Utilization of fly ash with silica fume and properties of Portland cement–fly ash–silica fume concrete. *Fuel* **2010**, *89* (3), 768–774 DOI: 10.1016/j.fuel.2009.10.003.
8. Estokova, A.; Kovalcikova, M.; Luptakova, A.; Prascakova, M. Testing Silica Fume-Based Concrete Composites under Chemical and Microbiological Sulfate Attacks. *Materials (Basel).* **2016**, *9* (5), 324 DOI: 10.3390/ma9050324.
9. Xu, W.; Lo, Y. T.; Wang, W.; Ouyang, D.; Wang, P.; Xing, F. Pozzolanic Reactivity of Silica Fume and Ground Rice Husk Ash as Reactive Silica in a Cementitious System: A Comparative Study. *Materials* . 2016.
10. Behfarnia, K.; Farshadfar, O. The effects of pozzolanic binders and polypropylene fibers on durability of SCC to magnesium sulfate attack. *Constr. Build. Mater.* **2013**, *38*, 64–71 DOI: 10.1016/j.conbuildmat.2012.08.035.
11. Chung, D. D. L. Improving cement-based materials by using silica fume. *J. Mater. Sci.* **2002**, *37* (4), 673–682 DOI: 10.1023/A:1013889725971.
12. ACI. Guide for the Use of Silica Fume in Concrete (ACI 234R-06). American Concrete Institute. **2006**.
13. Hooton, R. D. PERMEABILITY AND PORE STRUCTURE OF CEMENT PASTES CONTAINING FLY ASH, SLAG, AND SILICA FUME. In *ASTM Special Technical Publication*; 1986; pp 128–143.
14. Wolsiefer, J. T. Silica fume concrete: a solution to steel reinforcement corrosion in concrete. In *Utilization of Industrial By-Products for Construction Materials*; Publ by ASCE, 1993; pp 15–29.
15. Dotto, J. M. R.; Abreu, A. G. d.; Dal Molin, D. C. C.; Müller, I. L. Influence of silica fume addition on concretes physical properties and on corrosion behaviour of reinforcement bars. *Cem. Concr. Compos.* **2004**, *26* (1), 31–39 DOI: 10.1016/S0958-9465(02)00120-8.
16. Poon, C. S.; Kou, S. C.; Lam, L. Compressive strength, chloride diffusivity and pore structure of high performance metakaolin and silica fume concrete. *Constr. Build. Mater.* **2006**, *20* (10), 858–865 DOI: 10.1016/j.conbuildmat.2005.07.001.
17. Gjorv, O. E. Effect of condensed silica fume on steel corrosion in concrete. *ACI Mater. J.* **1995**, *92* (6), 591–598.
18. Ramezanianpour, A. A.; Malhotra, V. M. Effect of curing on the compressive strength, resistance to chloride-ion penetration and porosity of concretes incorporating slag, fly ash or silica fume. **1995**, *17* (2), 125–133 DOI: 10.1016/0958-9465(95)00005-W.
19. Neville, A. The confused world of sulfate attack on concrete. *Cem. Concr. Res.* **2004**, *34* (8), 1275–1296 DOI: 10.1016/j.cemconres.2004.04.004.

20. Al-Amoudi, O. S. B. Performance of 15 reinforced concrete mixtures in magnesium-sodium sulphate environments. *Constr. Build. Mater.* **1995**, *9* (3), 149–158 DOI: 10.1016/0950-0618(95)00007-3.
21. Baghabra Al-Amoudi, O. S. Attack on plain and blended cements exposed to aggressive sulfate environments. *Cem. Concr. Compos.* **2002**, *24* (3-4), 305–316 DOI: 10.1016/S0958-9465(01)00082-8.
22. Ganjian, E.; Pouya, H. S. Effect of magnesium and sulfate ions on durability of silica fume blended mixes exposed to the seawater tidal zone. *Cem. Concr. Res.* **2005**, *35* (7), 1332–1343 DOI: 10.1016/j.cemconres.2004.09.028.
23. Al-Dulaijan, S. U.; Maslehuddin, M.; Al-Zahrani, M. M.; Sharif, A. M.; Shameem, M.; Ibrahim, M. Sulfate resistance of plain and blended cements exposed to varying concentrations of sodium sulfate. *Cem. Concr. Compos.* **2003**, *25* (4-5), 429–437 DOI: 10.1016/S0958-9465(02)00083-5.
24. Lee, S. T.; Moon, H. Y.; Swamy, R. N. Sulfate attack and role of silica fume in resisting strength loss. *Cem. Concr. Compos.* **2005**, *27* (1), 65–76 DOI: 10.1016/j.cemconcomp.2003.11.003.
25. Hooton, R. D. Influence of silica fume replacement of cement on physical properties and resistance to sulfate attack, freezing and thawing, and alkali-silica reactivity. *ACI Mater. J.* **1993**, *90* (2), 143–151.
26. Cohen, M. D.; Bentur, A. Durability of Portland cement-Silica fume pastes in magnesium sulfate and sodium sulfate solutions. *ACI Mater. J.* **1988**, *85* (3), 148–157.
27. Türker, F.; Aköz, F.; Koral, S.; Yüzer, N. Effects of magnesium sulfate concentration on the sulfate resistance of mortars with and without silica fume. *Cem. Concr. Res.* **1997**, *27* (2), 205–214.
28. Santhanam, M.; Cohen, M. D.; Olek, J. Mechanism of sulfate attack: A fresh look. Part 1: Summary of experimental results. *Cem. Concr. Res.* **2002**, *32* (6), 915–921 DOI: 10.1016/S0008-8846(02)00724-X.
29. Ortega, J. M.; Esteban, M. D.; Rodríguez, R. R.; Pastor, J. L.; Ibanco, F. J.; Sánchez, I.; Climent, M. A. Influence of Silica Fume Addition in the Long-Term Performance of Sustainable Cement Grouts for Micropiles Exposed to a Sulphate Aggressive Medium. *Materials* **2017**, *10*, 890, doi:10.3390/ma10080890.
30. Williams, M.; Ortega, J. M.; Sánchez, I.; Cabeza, M.; Climent, M. A. Non-Destructive Study of the Microstructural Effects of Sodium and Magnesium Sulphate Attack on Mortars Containing Silica Fume Using Impedance Spectroscopy. *Appl. Sci.***2017**, *7*, 648, doi:10.3390/app7070648.
31. Asociación Española de Normalización y Certificación (AENOR). *UNE-EN 197-1:2011. Composición, Especificaciones y Criterios de Conformidad de Los Cementos Comunes;* AENOR: Madrid, Spain, 2011; p. 30. (in Spanish)
32. Asociación Española de Normalización y Certificación (AENOR). *UNE-EN 196-1:2005. Métodos de ensayo de cementos. Parte 1: Determinación de resistencias mecánicas*. AENOR: Madrid, Spain, 2005; p. 36. (in Spanish)
33. ASTM. *Standard Test Method for Length Change of Hydraulic-Cement Mortars Exposed to a Sulfate Solution ASTM C 1012-04*; ASTM International: Wesk Conshohocken, PA, USA, 2004; p. 6.
34. Andrade, C.; Alonso, C.; Arteaga, A.; Tanner, P. Methodology based on the electrical resistivity for the calculation of reinforcement service life. In *Proceedings of the 5th CANMET/ACO International Conference on Durability of Concrete, supplementary papers.*; Malhotra, V. M., Ed.; American Concrete Institute: Barcelona, Spain, 2000; pp 899–915.
35. Sánchez, I.; Nóvoa, X. R.; de Vera, G.; Climent, M. A. Microstructural modifications in Portland cement concrete due to forced ionic migration tests. Study by impedance spectroscopy. *Cem. Concr. Res.* **2008**, *38* (7), 1015–1025 DOI: 10.1016/j.cemconres.2008.03.012.
36. Cabeza, M.; Merino, P.; Miranda, A.; Nóvoa, X. R.; Sanchez, I. Impedance spectroscopy study of hardened Portland cement paste. *Cem. Concr. Res.* **2002**, *32* (6), 881–891 DOI: 10.1016/S0008-8846(02)00720-2.
37. Ortega, J. M.; Sánchez, I.; Climent, M. A. Impedance spectroscopy study of the effect of environmental

conditions on the microstructure development of sustainable fly ash cement mortars. *Materials.* **2017**, *10* (10) DOI: 10.3390/ma10101130.

38. Pastor, J. L.; Ortega, J. M.; Flor, M.; López, M. P.; Sánchez, I.; Climent, M. A. Microstructure and durability of fly ash cement grouts for micropiles. *Constr. Build. Mater.* **2016**, *117*, 47–57 DOI: 10.1016/j.conbuildmat.2016.04.154.
39. Ortega, J. M.; Esteban, M. D.; Rodríguez, R. R.; Pastor, J. L.; Ibanco, F. J.; Sánchez, I.; Climent, M. A. Long-Term Behaviour of Fly Ash and Slag Cement Grouts for Micropiles Exposed to a Sulphate Aggressive Medium. *Materials* **2017**, *10*, 598. doi:10.3390/ma10060598
40. Keddam, M.; Takenouti, H.; Nóvoa, X. R.; Andrade, C.; Alonso, C. Impedance measurements on cement paste. *Cem. Concr. Res.* **1997**, *27* (8), 1191–1201 DOI: 10.1016/S0008-8846(97)00117-8.
41. Ortega, J. M.; Sánchez, I.; Antón, C.; De Vera, G.; Climent, M. A. Influence of environment on durability of fly ash cement mortars. *ACI Mater. J.* **2012**, *109* (6), 647-656.
42. Ortega, J. M.; Sánchez, I.; Climent, M. A. Durability related transport properties of OPC and slag cement mortars hardened under different environmental conditions. *Constr. Build. Mater.* **2012**, *27* (1), 176–183 DOI: 10.1016/j.conbuildmat.2011.07.064.
43. Duan, P.; Shui, Z.; Chen, W.; Shen, C. Effects of metakaolin, silica fume and slag on pore structure, interfacial transition zone and compressive strength of concrete. *Constr. Build. Mater.* **2013**, *44*, 1–6 DOI: 10.1016/j.conbuildmat.2013.02.075.
44. Aköz, F.; Türker, F.; Koral, S.; Yüzer, N. Effects of sodium sulfate concentration on the sulfate resistance of mortars with and without silica fume. *Cem. Concr. Res.* **1995**, *25* (6), 1360–1368 DOI: 10.1016/0008-8846(95)00128-Y.
45. Al-Dulaijan, S. U. Sulfate resistance of plain and blended cements exposed to magnesium sulfate solutions. *Constr. Build. Mater.* **2007**, *21* (8), 1792–1802 DOI: 10.1016/j.conbuildmat.2006.05.017.